Macromolecules

Article

Cite This: Macromolecules 2019, 52, 2521−2530

pubs.acs.org/Macromolecules

Diluting Entangled Polymers Affects Transient Hardening but Not Their Steady Elongational Viscosity

Taisir Shahid,[†,‡] Christian Clasen,[‡] Filip Oosterlinck,[§] and Evelyne van Ruymbeke*[,†]

[†]Bio and Soft Matter, Institute on Condensed Matter and Nano-science, Université catholique de Louvain, Louvain-la-Neuve, Belgium

[‡]Department of Chemical Engineering, KU Leuven, Celestijnenlaan 200f, 3001 Leuven, Belgium

[§]DSM Materials Science Center, P.O. Box 18, NL-6160 MD Geleen, The Netherlands

ABSTRACT: It is now established that the huge qualitative difference in flow behavior between entangled polymer melts and solutions in nonlinear elongational flows cannot be explained in the framework of the "standard" tube model. Instead, the additional relaxation mechanism of alignment-induced friction reduction, acting primarily in melts, has shown its interesting potential to explain the experimental data. Here, we critically assess this mechanism by means of a systematic experimental investigation of the extensional response of long polystyrene chains diluted in short chain matrices of varying molar mass, varying the interaction between long chains and their molecular environment. We find that, surprisingly, all polystyrene blends exhibit different transient strain hardening properties but the same apparent steady-state elongational viscosity; i.e., the long chains reach the same final stretch state as long as the short chain exceeds a critical molar mass of about 4 kg/mol, well below the entanglement limit, and do not significantly contribute to the strain hardening. This observation contradicts, in part, the basic assumption according to which the elongation state of a chain depends on its molecular environment, and raises new fundamental questions, in particular on the relationship between transient strain hardening and the stretch state of the chains and its consequences on the nonuniversal behavior of melts and solutions in strong flows.

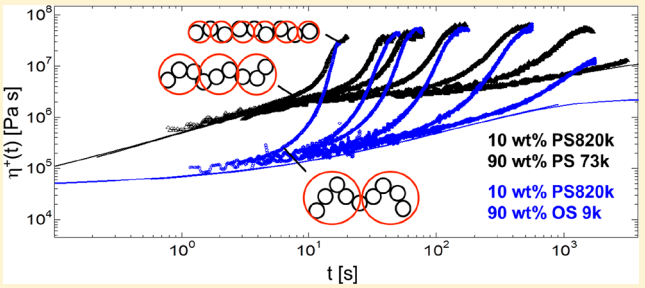

I. INTRODUCTION

Predicting the linear viscoelastic (LVE) properties of monodisperse polymers has reached a quantitative level based on mesoscopic approaches such as slip-link models[1−11] or the Doi−Edwards tube-model theory[12] combined with established relaxation mechanisms such as reptation, contour length fluctuations, and constraint release (CR).[13−17] The latter mechanism is particularly important for binary blends since it describes the influence of fast relaxation of shorter chains on the relaxation of longer chains.[18−20] Despite the fact that predicting the flow properties of such blends remains one of the main challenges for tube models,[21−23] a consistent molecular picture could be proposed for describing the linear regime, which allows explaining the different experimental data based on the same framework.[21] In particular, in the case of polymer chains diluted in an oligomer matrix, the universality of linear viscoelastic response of polymers was demonstrated with different chemical structures and concentrations, as long as the chains have the same number of entanglements.[13,24,26,27] However, it was shown recently that the universality between polymer melts and solutions breaks down under nonlinear elongational flows:[25,26] while polymer melts exhibit a monotonic extension-thinning behavior for all applied strain rates,[29] polymer solutions with the same number of entanglements exhibit an initial thinning behavior followed by a strong extension hardening, which occurs at rates comparable to the reciprocal Rouse time of the chains.[28] As a result, molecular theories for linear flows cannot be extended to nonlinear flows without further considerations.

This nonuniversality is now well established experimentally; however, its molecular origin and in particular the absence of an extension thickening for polymer melts are not yet fully understood.[29,30] This indicates that there is an important relaxation mechanism missing in polymer physics. Marrucci and Ianniruberto[31] proposed a first explanation, which is a flow-induced contraction of the tube diameter from its equilibrium, that ultimately results in a pressure-induced relaxation effect. Known as the interchain pressure concept, it includes a novel nonlinear parameter: the tube diameter relaxation time, τ_a. By incorporating this concept in the molecular stretch function theory, Wagner et al.[32] were able to attain a semiquantitative agreement for monodisperse PS melts[29] and showed that the tube diameter relaxation time scales with the Rouse time of the chains. Later, this work was successfully extended to entangled chains diluted in oligomers[33] and small molecule solvents.[34] However, this

Received: December 19, 2018
Revised: February 3, 2019
Published: March 14, 2019

DOI: 10.1021/acs.macromol.8b02701
Macromolecules 2019, 52, 2521−2530

required using two different Rouse times for the melt and the solution state,[35] which is difficult to comprehend. Furthermore, with binary blends of monodisperse linear chains, it was shown that τ_a varies with the weight ratio of long to short chains in the blend, which should not be the case if it is related to a Rouse process.[36]

Recently, it was proposed[37] that the monotonic thinning behavior observed in the melt state is due to an alignment-induced reduction of the monomeric friction under fast elongational flow.[38,39] This mechanism calls for a stretching of the chains in fast flows, inducing strong local anisotropy and resulting in a decrease of the (monomeric) friction coefficient of the chains. A priori, this should mainly affect entangled polymer melts, since in solution the small molecules do not align.[38] However, a recent work by Huang et al.[40] suggests that in oligomeric solution friction reduction can also take place due to nematic interactions[41−43] between the oligomers and the polymer molecules and with the importance of this process increasing with the size of the oligomers. Subsequently, a nematic interaction parameter ε was included in the nonlinear tube model,[44] defined as the ratio of the order parameter of the short molecules to the average order parameter of the system. The resulting model allowed obtaining a more accurate description of the properties of various polystyrene (PS) melts and solutions.[44−46] Very recently, Park and Iannirubertо[46] established the dependence of ε on the molar mass of PS oligomers. Four different regions were distinguished as shown in Figure 1. Initially, ε increases with the oligomer

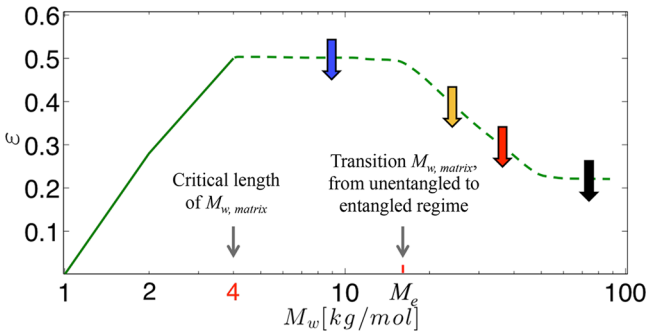

Figure 1. Nematic interaction parameter, ε, vs styrene molar mass, M_w. The dashed part of the curve is hypothetical.[46] The M_w of the PS matrices used in this study (symbols) were chosen to explore all three hypothetical regimes.

molar mass (for $M \ll M_e$), followed by a regime where ε is constant (up to $M \approx M_e$). Then ε decreases and finally becomes constant when the chains are fully entangled. Only the first regime has been observed experimentally,[40,46] whereas the other regimes are not yet confirmed, with the exception of the work of Ylitalo et al.[47] (for polybutadiene).

However, this is in contrast to the work of Tassin et al.,[45] who found a constant value of ε for 10 and 27 kg mol^{-1}styrene oligomers, and to the work of Doi et al.,[46] who showed that nematic interaction has only a small effect on the viscoelastic properties, although it can be strong for the optical properties. On the other hand, the validity of reduced friction upon large flow is also questioned by results obtained with specific slip-link models such as the one proposed by Andreev et al., which also shows deviations from the experimental data, but in the opposite direction,[10] thus leading to a larger discrepancy if a reduced friction is considered. It must be noted, however, that other slip-link models, such as the multichain approach proposed by Yaoita et al.[25] or the model of Takimoto and Doi,[50] show the opposite trend, i.e., a pronounced hardening in blends of long chains with short chains.

From the above it is evident that role of oligomer size on the extension-hardening reduction, and its consequences on advancing the state-of-the-art in polymer physics in the direction of developing molecular constitutive equations, represents an outstanding challenge. In this paper we address this challenge with a systematic data set, based on carefully designed experimental systems, that allows exploring the transition from polymer melts to polymer solutions in uniaxial extension by means of long PS chains diluted in matrices of oligomers of different sizes. To this end, long chain PS is diluted at equal concentrations in polystyrene matrices of different molar mass, $M_{w,matrix}$, ranging from unentangled to fully entangled states. These samples have been selected to ensure that friction reduction due to changes in configuration is solely governed by the suggested long chain−matrix nematic interaction, i.e., the reciprocal Rouse times of the matrices exceed the elongation rates, so that the short chains do not stretch over the entire range of our experiments (see details in the Appendix).

The results provide the needed ingredients to understand why and how the transition from polymer−oligomer to polymer−polymer interaction affects the strain hardening behavior. Indeed, the experimental data suggest that all PS blends have the same apparent steady elongational viscosity when compared at same distance in temperature from their glass transition temperature, T_g. This observation leads us to the conclusion that as long as the matrix exceeds a "critical molar mass" (around 4 kg/mol[40]), the long chains/matrix nematic interaction is not present or at least is constant and independent of the molar mass and entanglement state of the matrix molecules. In addition, the departure of the transient viscosity curves from their linear viscoelastic (LVE) envelopes is much more pronounced in an oligomeric matrix than in an entangled matrix, demonstrating the large influence of partial relaxation of the longer matrix chains on transient strain hardening. These results raise thus new questions on the physics of the polymeric response in strong flows.

II. EXPERIMENTAL DETAILS

Four different blends were prepared by diluting a long PS chain (PS820) at a concentration of 10 wt % in four different matrices (from Polymer Source, Montreal, Canada). The long component was always self-entangled. The short chains ranged from oligomers (OS9) to a fully entangled state (PS73), but they never stretched at the particular experimental conditions. Their weight-average molar mass M_w and polydispersity PDI were assessed by gel permeation chromatography, and for PS820 by field flow fractionation coupled with multiangle light scattering (at BASF, Germany), yielding 820 kg mol^{-1} and 1.02 for PS820; 8.8 kg mol^{-1} and 1.11 for OS9; 23 kg mol^{-1} and 1.09 for PS23; 34 kg mol^{-1} and 1.11 for PS34; and 73 kg mol^{-1} and 1.08 for PS73.

The PS blends were prepared following a four-step procedure inspired by an earlier work.[27] In this procedure, first the polystyrene and the oligomer are weighted according to the desired weight fractions and dissolved together in THF. The mixture is then stirred at room temperature overnight to ensure that the components are well dissolved and mixed. In a next step, the whole mixture is added to a nonsolvent (methanol) drop by drop, using a buret. The precipitated polymer/oligomer blend is then separated and collected using paper filtration. Finally, the blends are dried at high temperatures under vacuum to remove any remaining traces of the solvents.

DOI: 10.1021/acs.macromol.8b02701
Macromolecules 2019, 52, 2521−2530

Table 1. Main Characteristics of the Blends

	blend composition	Z_L/Z_S	T_g [°C]	exptl temp, T [°C]	τ_R (matrix) at T_g + 31.4 °C [s]
B1	10% PS820−90% PS73	54/5	106.6	138	2.9
B2	10% PS820−90% PS34	54/2	104.7	136	0.63
B3	10% PS820−90% PS23	54/1	103.5	135	0.29
B4	10% PS820−90% OS9	54/<1	98.6	130	0.04

The presence of solvent can profoundly alter the strain hardening behavior of the PS samples. Thus, extra cautions were taken to ensure that the samples are free from any sort of impurities. For this, the PS blends were dried inside a vacuum oven at a temperature higher than the melting temperatures of the solvents and close to the glass transition temperature of the PS blends. Both THF and methanol have a melting temperature of around 65 °C, while the glass transition temperature of the PS systems is ∼100 °C. Therefore, the PS blends were first dried at 90 °C for several hours and then at 70 °C for about a week. It should be noted that the samples were dried as powders rather than in solid blocks to ensure an easier diffusion of the solvent.

The quantity of THF added in the first step influences the final form of the mixture. Therefore, this quantity was tuned to obtain PS mixture in fine powder form, thus making it easier to evaporate the residual solvents.

The main characteristics of the blends are listed in Table 1. The number of entanglements along the long and short chains (Z_L and Z_S, respectively) and the isofrictional Rouse relaxation time of the matrix (τ_R) are also given (details in the Appendix). T_g was determined by differential scanning calorimetry.

Because the longest chain PS (PS820) was diluted at same concentration (10 wt %) but in in the short chain matrices of different lengths, the T_g of each blend was found to vary, depending on the molar mass of the short components. This difference in T_g values must be taken into account to allow a comparison of the viscoelastic responses. This can be achieved by working under iso-T_g conditions,[55] i.e., by keeping the same temperature difference between the experiment and the glass transition temperature of each blend. Working at iso-T_g condition is in particular important for amorphous polymers such as PS because of its high T_g (∼100 °C) and therefore the relatively low temperature difference between the glass transition and the experimental temperature.

The LVE properties were measured by small-amplitude oscillatory shear tests performed on a MCR 301 (Anton Paar, Austria) rheometer using a stainless steel parallel plate geometry (with a diameter of 8 mm), with a convection oven for temperature control (∼0.1 °C) under constant nitrogen gas supply. After an amplitude sweep to determine the LVE region, frequency sweep tests were performed at three different temperatures (ranging from 130 to 170 °C for samples B1−B3 and from 120 to 160 °C for sample B4 with lower T_g) and shifted onto a single master curve at a reference temperature T_{ref}, using time−temperature superposition (TTS).[54] These master curves were then brought to iso-T_g conditions ($T_{ref} - T_g$ = 31.4 °C)[55] by shifting horizontally and ensuring a good overlap of the viscoelastic response in the high-frequency region, in which the chain relaxation is controlled by local Rouse dynamics and thus depends only on ($T_{ref} - T_g$). As discussed below, the validity of the shift factors to this specific reference temperature can then be confirmed by comparing their value to the shift factors versus temperature curve used to build the different TTS master curves for different blends.

The shifted iso-T_g data measured at 120 °C (for blend B4) or 130 °C (for blends B1−B3) are then used as reference curves to shift the other experimental data measured at higher temperatures and to create general master curves. It should be noted that no vertical shift has been considered here, since the range of temperatures used is rather limited. In Figure 2, all shift factors used to create the master curves are plotted against ($T - T_g$). As it can be seen, when plotted in such a way, the values used for the PS blends nicely coincide with each other and the WLF equation for melts and entangled chains diluted in oligomer matrix[26,27]

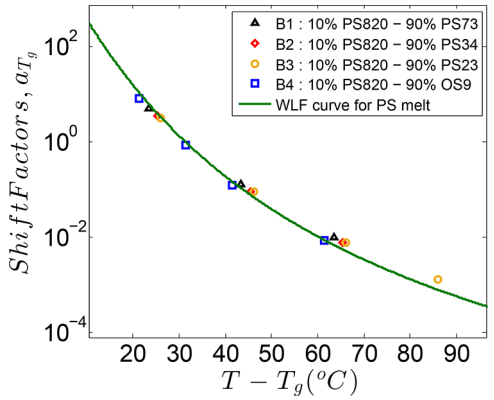

Figure 2. Time−temperature superposition shift factors as a function of ($T - T_g$), determined for the different polymer blends. The continuous curve represents the WLF equation used in ref 1.

$$\log a_T = \frac{-c_1^0(T - T_{ref})}{c_2^0 + (T - T_{ref})} \quad (1)$$

where c_1^0 = 8.19, c_2^0 = 89.53 K, T_{ref} = 138 °C, and T, the temperature, is expressed in °C. The fact that all these curves superimpose also validates the factors used for shifting the data under iso-T_g conditions. Furthermore, this good agreement, together with a good overlap of the high frequency data in the storage and loss moduli curves, validates the values experimentally found for T_g.

Note that the WLF curve used in this work is in good agreement with the one proposed in previous works.[26,27]

Transient elongational stress measurements were performed with a filament stretching rheometer (VADER-1000, Rheo Filament, USA) using a stainless steel parallel plate geometry (with a diameter of 6 mm), with an oven for temperature control (∼0.1 °C) under constant nitrogen gas supply. Prior to the measurements, all samples were dried under vacuum at 65 °C overnight. These samples were then molded into discotic specimens with a fixed radius of 2.75 mm using a homemade mold under vacuum. The samples were pressed at 140−150 °C and annealed at the same temperature (at least 20 min) under vacuum. A three-step protocol was followed: first, the sample was slightly squeezed at 150−160 °C to ensure adequate contact between the sample and the plates. Next, the sample was prestretched to a smaller radius R_0 ranging from 1 to 2.5 mm (to reduce the risk of sample detachment during the next step). Finally, the temperature was decreased to the experimental temperature ($T - T_g$ = 31.4 °C, see Table 1), and subsequently the time-dependent stress growth coefficient was measured at constant Hencky strain rates between 0.001 and 0.2 s^{-1}. The importance of working under iso-T_g conditions, as well as further details on the measurement protocol, are presented in the Appendix.

III. RESULTS AND DISCUSSION

The linear and nonlinear responses of the PS blends are shown in Figures 3 and 4, respectively. The tube-based model used to predict the LVE properties of the blends is discussed briefly in the Appendix.

The LVE data clearly show a fast relaxation of the short matrix at high frequencies, followed by the relaxation of the long chains at lower frequencies. While the short chains in

DOI: 10.1021/acs.macromol.8b02701
Macromolecules 2019, 52, 2521−2530

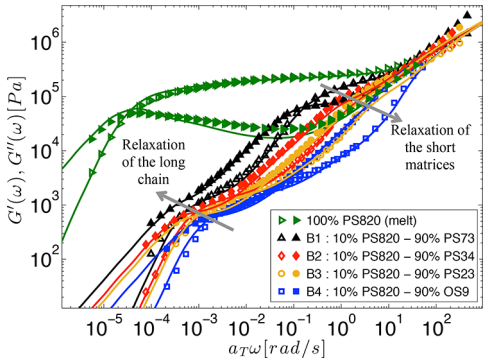

Figure 3. Experimental (symbols) and predicted (lines) storage (open symbols) and loss (closed symbols) moduli of the PS blends at iso-T_g conditions.

sample B1 with about five entanglements form a rubbery plateau, the breadth of this plateau gradually diminishes with shorter matrix molecules, and it eventually disappears for blend B4. Despite the fact that the same concentration of long chains is used for all blends, their terminal relaxation time decreases with decreasing length of the matrix due to a larger CR effect.[19,20,27] These experimental data are used to create the LVE envelopes for the elongational data of Figure 4. Any upward deviation from these envelopes is a signature of transient strain hardening (SH). As already mentioned, the observed SH results entirely from the stretching of the long chains (see Figure 6) but is influenced by their interaction with the different matrices. The Hencky strain rates are also low enough to ensure that the short matrices do not orient with the flow (with their inverse reptation time shorter than the highest strain rate), except for the long chains blended to the longest matrix, PS73, and deformed at the highest strain rate (0.02 s^{-1}). It should be noted that in this work the term "steady elongational viscosity" represents the constant elongational viscosity reached by the transient viscosity curve after a certain time but does not especially refer to a steady state.[51−53]

We first interpret the extend of SH with the established approach, i.e., via the deviation from the linear envelope and by comparing normalized curves with respective LVE envelopes (Figure 4b).[26,40,57,58] While all blends depict strong transient strain hardening, the deviation from the LVE envelope is reduced with increasing $M_{w,matrix}$. A similar trend, going from polymer solution to melt, has been reported in the literature[26] and was attributed to the above-mentioned stretch-induced friction reduction. However, this explanation cannot hold for the present samples since the matrices are not stretched (see Figure 6). The alternative scenario is the monomeric friction reduction due to enhanced nematic interactions. In such a case, by looking at the importance of the transient strain hardening (Figure 4b), the results would suggest that ε increases monotonically with $M_{w,matrix}$ even when the matrix is fully entangled. This raises a first issue: the interpretation of the data is physically questionable, since it is clear that nematic interactions cannot be enhanced in entangled polymer melts. In fact, from the analysis of the non-normalized data (Figure 4a), we would rather conclude that in this range of molar masses ($M_{w,matrix}$ > 4 kg/mol) the nematic interaction parameter is constant. This highlights the importance of correctly interpreting the data and to re-examine the meaning of transient strain hardening. Furthermore, our results contradict the hypothetical decrease of the nematic interaction

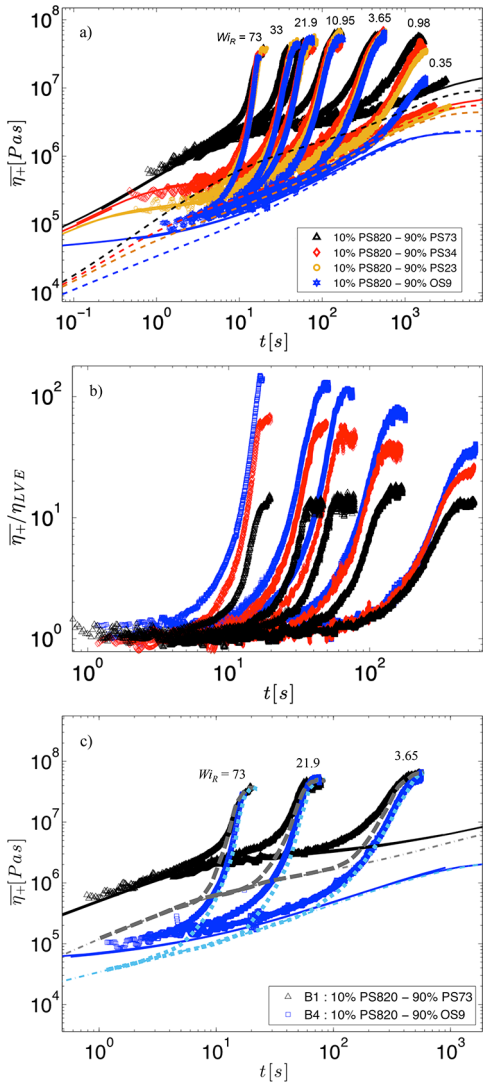

Figure 4. (a) Transient response of PS blends under elongational flow at various rates as indicated. Solid lines are the LVE envelopes, while the dashed lines are predictions of the contribution of long chains to the LVE envelop. Slight discrepancy at short times with highest W_{iR} (defined with respect to the long chain) is discussed in the Appendix. (b) Responses of blends B1, B2, and B4 are normalized by the corresponding LVE data in elongation, which have been estimated from the complex viscosity, such as $\eta_{LVE}(t) = 3\eta(\omega = 1/t)$ (blend B3 is excluded for clarity). (c) Transient response of blend B1 (black and gray) and blend B4 (blue and light blue) sample. Experimental elongation curves (symbols) are compared to the full LVE envelopes (solid lines) and to the long chain LVE (dash-dotted curves; estimated from model). Dashed curves are drawn to illustrate the onset of long chain stretching. (for clarity, only blends B1 and B4 are shown).

parameter with increasing molar mass of the matrix, as it was proposed by Ylitalo et al.[47] and Park and Ianniruberto[46] in the case of high molar mass matrix ($M_{w,matrix} > M_e$, see Figure 1). While previous works[40,46] have experimentally shown that nematic interactions have a large influence on the elongation behavior of long chains diluted in very short matrices ($M_{w,matrix}$ < 4 kg/mol), the experimental data presented here allow us to complete this picture for larger molar masses ($M_{w,matrix}$ > 8 kg/mol) and to show that in such a case nematic interactions are constant.

DOI: 10.1021/acs.macromol.8b02701
Macromolecules 2019, 52, 2521−2530

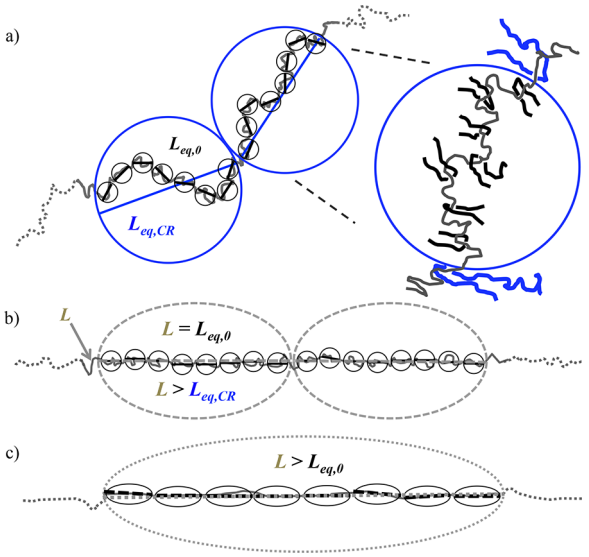

Figure 5. (a) Relaxation state reached by the long chain through the CR process before stretch occurs. The black blobs correspond to the initial entanglement segments, with a corresponding primitive path of length $L_{eq,0}$, while the blue blobs correspond to their equilibrium state after the CR process, with a corresponding primitive path of length $L_{eq,CR}$. (b) Chain conformation corresponding to $L/L_{eq,0}$= 1: It represents the transition state at which $\lambda_{CR} = L/L_{eq,CR} > 1$ while $\lambda = L/L_{eq,0} = 1$. (c) Onset of stretch $\lambda = L/L_{eq,0} > 1$ (shown for one long–long entanglement blob).

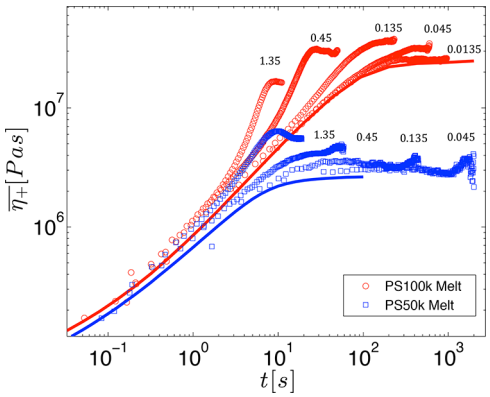

Figure 6. Transient response (symbols) of PS melts, coming from ref 29. Solid lines represent the linear viscoelastic envelopes. Strain rates are shifted to ΔT_g = 31.4 °C from 23.4 °C.

As already mentioned, defining SH as typically done in the literature[26,40,57,58] with respect to the LVE envelope raises concerns in the case of blends. This is partially due to the fact that the entanglement state of the linear matrix may strongly affect the LVE response. Consequently, we expect that part of SH coming from the long chains is masked by the viscoelastic response of the matrix itself, especially if the latter takes time to relax. To rationalize this effect, we used the tube model[59] to extract the contribution of the long chains to the LVE envelope of the blend, which is depicted with dotted lines in Figure 4a. Comparing this to the measured LVE envelope of the blend (solid lines), it becomes evident that for samples B1–B3 the long chain stretching should start well below the level of the full LVE envelope (illustrated further in Figure 4c) but is masked by the matrix contribution. In contrast to this, for sample B4 the oligomer matrix relaxes fast enough and contributes only weakly to the LVE envelope, so that the SH arising from the long chains is fully detectable and appears to be stronger. Therefore, the LVE envelopes influence the way the curves are normalized and consequently the final level of SH (Figure 4b). These observations demonstrate the large effect of the linear response on the actual magnitude of SH and justify an alternative way proposed in the following to quantify the actual stretch state of the long chains in a way that is independent of the LVE properties of the blends.

To achieve this, we directly relate the final long-chain stretching to the steady values of the elongational stress growth curves, as the short component has no effect at this level (given the choice of $M_{w,matrix}$ and $\dot{\varepsilon}$), and all blends contain the same weight ratio of long to short chains. Interestingly, it is observed that all tested PS blends reach the same apparent steady-state value (for $W_{iR} = \dot{\varepsilon}\tau_{Rouse} > 1$), implying that the particular choice of matrix chains has no impact on the final stretch of the long chains. We can then conclude that beyond a "critical molar mass" of the matrix (of about 4 kg/mol[40]), the polymer–matrix interaction has no effect or at least remains unaltered and friction reduction does not depend on the length of the matrix chains anymore. This unambiguous experimental observation contradicts thus the behavior proposed in Figure 1.

These results also illustrate the large ambiguity in relating the extent of transient SH (i.e., departure from linear envelope) to the stretch state of the chains: while Figure 4a suggests that the long chains reach the same steady-state stretch level, and hence the same final SH (i.e., elongational viscosity), the transient SH shown in Figure 4b strongly decreases with $M_{w,matrix}$.

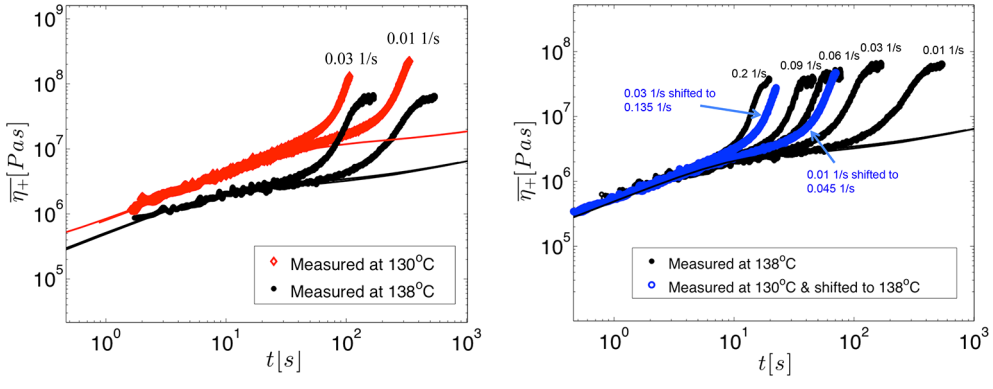

Figure 7. Left: blend B1 measured at different temperatures. Right: data shifted according to the TTS shift factor.

DOI: 10.1021/acs.macromol.8b02701
Macromolecules 2019, 52, 2521–2530

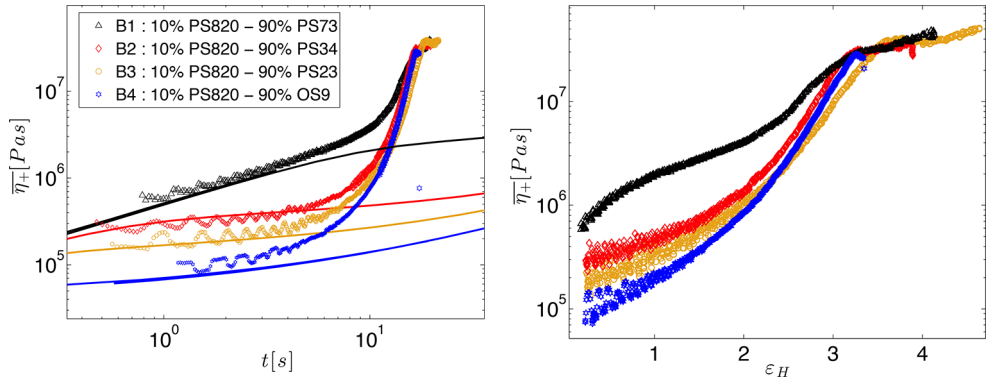

Figure 8. Transient elongational viscosity at W_{iR} = 73.

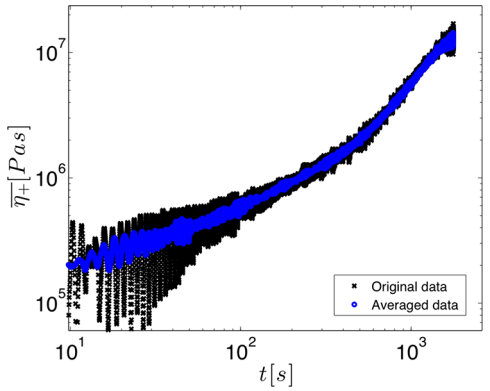

Figure 9. Comparison between measured and averaged data for blend B4 at 0.003 s^{-1}.

Table 2. Main Characteristics of Different Components of the Blends

mol wt [kg/mol]	Z	PDI	T_g [°C]
820	54	1.02	106.6
73	5	1.08	105.6
34	2	1.11	103.3
23	1	1.09	92.4
8.8	<1	1.1	94.6

As already discussed, this large difference in transient hardening mainly comes from the LVE response of the matrix, which masks the initial SH of the long chains. But this is not the only reason: Even if we compare the data with the LVE of the long chains estimated from our tube model (see Figure 4c), the transient SH still decreases with increasing $M_{w,matrix}$. This is due to a second process that influences transient SH, namely, the capability of the long chains to partially relax before starting to stretch. Indeed, long chains diluted in a fast-relaxing matrix will rapidly relax a part of their orientation through the CR process, since the continuous loss/creation of entanglements with short chains enables them to explore a larger effective tube diameter, $a_{CR}(t)$, defined as

$$a_{CR}(t) = a_0\phi(t)^{-\alpha/2} \tag{2}$$

where a_0 is the initial tube diameter (i.e., accounting for all initial short−long and long−long entanglements), $\phi(t)$ is the dilution factor, and α is the dynamic dilution exponent, which has been fixed to 1, consistent with our previous work.[20,23,27]

As illustrated in Figure 5a, another consequence of the CR process is the reduction of the effective length of the primitive path, $L_{eq,CR}(t)$, of these long chains:

$$L_{eq,CR}(t) = L_{eq,0}\phi(t)^{\alpha/2} \tag{3}$$

where $L_{eq,0}$ represents the initial length of the primitive path, i.e., before the relaxation of the short chains.

It is important to note here that while the equilibrium length of the long component, $L_{eq,0}$, is constant for all PS blends, the time scale at which $L_{eq\text{-}CR}(t)$ decreases strongly depends on the matrix relaxation time. It is also important to note that the transient SH appears as soon as the stretch factor $\lambda_{CR}(t) = L(t)/L_{eq,CR}$, which compares the real length of the primitive path, $L(t)$, to its effective equilibrium length, $L_{eq,CR}$, takes on values >1.[30] Consequently, the importance of transient SH increases with the efficiency of the CR process, i.e., with decreasing the molar mass of the short component. In other words, if the long chains have time to relax by CR before starting to stretch, they will have a larger "reservoir" of deformation and their transient strain hardening will be more important. Because of the shorter length of their primitive path, $L_{eq,CR}$ (see Figure 4c), long chains diluted in a fast relaxing matrix also start to show transient strain hardening before the same long chains diluted in a longer matrix.

On the basis of this result, we propose to distinguish two different stretch regimes: The first one starts at time t_{SH}, at which the elongation curves depart from the linear envelop (i.e., $L(t_{SH}) > L_{eq,CR}(t_{SH})$). In this regime, the stretch factor $\lambda(t) = L(t)/L_{eq,0}$ (which is defined as a function of the initial length of the tube) is still equal to 1 (see Figure 5b), while $\lambda_{CR}(t)$ is already taking on larger values, leading to SH. When the deformation is increased further (see Figure 5c), the curves enter the second stretch regime, in which λ is also becoming larger than 1. In this regime, as it can be observed in Figure 4a, the evolution of $\lambda(t)$ with time is identical for all samples. Because the same long chains in the same weight ratio of long to short chains are used for all blends, which all reach the same apparent steady viscosity, this indicates that the evolution of $L(t)$ is identical for all samples. However, the stretch factor $\lambda_{CR}(t)$ stays different, since its starting point, $L_{eq,CR}(t_{SH})$, depends on the short matrix:

$$\lambda_{CR}(t) = \frac{L(t)}{L_{eq,CR}(t_{SH})} = \frac{L(t)}{L_{eq,0}}\frac{L_{eq,0}}{L_{eq,CR}(t_{SH})} = \lambda(t)\frac{L_{eq,0}}{L_{eq,CR}(t_{SH})} \tag{4}$$

As already mentioned, λ_{CR} increases with decreasing $M_{w,matrix}$, leading to an enhancement of the transient SH (see Figure 4a).

DOI: 10.1021/acs.macromol.8b02701
Macromolecules 2019, 52, 2521−2530

Thus, one can say that the length of the long chains primitive path, $L(t)$, increases independently from its molecular environment, while the importance of transient strain hardening depends on the relaxation state of the long chains at the time $t = t_{SH}$ at which $L(t)$ becomes longer than $L_{eq,CR}(t)$. Because this last process strongly depends on the sample composition, the importance of transient strain hardening also varies a lot (see Figure 4b). The results illustrate the key role of the matrix for the transient SH and are expected to have large consequences for blends in which the weight ratio of long to short chains is varied.

It must be noted that the picture proposed here most probably fails at very high Hencky strain rates, at which the chains are close to their finite extensibility. Indeed, in such a case, the entanglement segments (defined in the initial or in the dilated tube) lose their Gaussian properties and do not behave as Hookean spring anymore. Because the strain rates applied are rather low (i.e., such as the monomeric equilibration has time to take place along molecular segments of around 100 kg/mol), we believe the chains do not reach this finite limit.

IV. CONCLUSION

In conclusion, we have demonstrated that above a critical molar mass (of ∼4 kg/mol[40] for PS) polymer−matrix interactions remain unaltered, and the size of the matrix does not play a role anymore on the final stretching of the long chains. Our results put the existing framework for understanding polymer stretching into question and provide new insight into the components relevant for the actual SH process: there exists a clear distinction between transient strain hardening and final stretching of the long chains that determines the steady-state elongational viscosity. The former strongly depends on the polymer matrix, whereas the latter depends solely on the elongation rate (as well as the long chain M_w and concentration). This distinction is important for the fundamental understanding of the transition from polymer melts to polymer solutions under extensional flow and will have consequences in our continuing quest to establish a universal framework describing viscoelastic behavior under strong flows.

APPENDIX

A. Rouse Time of the Short Chains Matrix and Related Stretch State

In this section, the different characteristics of PS blends (as presented in Table 1) are defined. The number of entanglements along the short and long chains was calculated from the ratio of the molar mass of the corresponding component and the molar mass between entanglements, $Z = M_w/M_e$. Following our previous works, the value of M_e is fixed to 15 kg/mol.[27]

The Rouse time, which is the longest relaxation time of an unentangled chain, is important in elongational flow as polymer chains are presumed to be stretched when the flow rate exceeds the reciprocal of this characteristic time. In a typical tube model, this relaxation time is defined as $\tau_{Rouse} = \tau_e Z^2$, where τ_e is the relaxation time of a molecular segment between entanglements.[5] The value of τ_e depends on the iso-T_g condition, and in this work it is set to 0.12 s at $\Delta T_g = 31.4$ °C, in agreement with our previous works.[27] Consequently, the short chains should start to stretch at strain rates of $1/\tau_{Rouse}$, i.e., 0.35, 1.59, 3.45, and 25 s^{-1} for matrices of molar masses equal to 73, 34, 23, and 8.8 kg/mol, respectively, while PS820 starts to stretch are strain rate of 2.8×10^{-3} s^{-1}. To avoid stretching of the short components, the highest strain rate used in this work is 0.2 s^{-1}.

Because chain stretching depends on the Rouse time of the chains, it is important to accurately determine the actual value of this time. However, it has been shown that this value can vary up to a factor 2, depending on the used model.[56] If the Rouse time was 2 times shorter than the proposed values, this would not affect the results. On the other hand, if it was 2 times longer, this would mean that the short chains should start to stretch at 0.175, 0.8, 1.73, and 12.5 s^{-1} for matrices of molar masses of 73, 34, 23, and 8.8 kg/mol, respectively. We see that in such a case all samples stay below their stretch limit, apart from the longest matrix (73 kg/mol), when deformed at the highest strain rate. Thus, even with this uncertainty, the picture proposed here is still valid.

The fact that strain rates selected here do not lead to strain hardening of the matrix can be further validated by looking at literature elongational data of PS melts[29] similar to the ones used in this work. In Figure 6, it is observed that a PS melt with a molar mass of 50 kg/mol does not show strain hardening (which results from stretch of chains) at strain rates lower than 0.4 s^{-1}, while a PS melt with a molar mass of 100 kg/mol starts to strain harden at rates above 0.13 s^{-1}. This last strain rate corresponds to a critical rate of $(0.13\ s^{-1}\left(\frac{100}{70}\right)^2 =) 0.265\ s^{-1}$ in the case of polymer chains of mass equal to 70 kg/mol. This value is indeed above the maximum Hencky strain rate used in this work.

B. Importance of Working under Iso-T_g Conditions

All uniaxial extension measurements were performed at iso-T_g conditions as mentioned in Table 1. This is important as the T_g of blends containing the highest and lowest $M_{w,matrix}$, B1 and B4, differs almost by 8 °C. This temperature difference can't be ignored, especially for PS, whose activation energy is very high, so that even a small change in temperature can cause strong variations in its viscoelastic properties as shown in Figure 7 (left).

An alternative way of measuring at iso-T_g conditions is to measure the blends at the same temperature and then shift using the TTS shift factors, as mostly done in the literature (also shown in Figure 7 (right). However, to avoid any shifting (which might induce a certain degree of error), in this work all measurements are done at the same iso-T_g conditions.

C. Experimental Issues

i. Influence of Sample Prestretching. For blend B4, there is a slight deviation from the LVE envelope for high strain rates at low times. Owing to its high strain-hardening nature, the blend B4 had to be prestretched more to avoid detachment of sample from the plates (due to a high force buildup). This prestretch can result in residual stresses, which take a longer time to relax. However, this phenomenon only influences the data at short times. The steady value at long times are unaffected, as the stress involved is a few orders of magnitude higher.

It must be noted that we could not measure the elongational properties of the pure sample PS820. Indeed, this highly viscous sample requires an important prestretching to avoid its detachment. Consequently, an equilibration time of around 6 h at 170 °C is needed, which leads to sample degradation.

DOI: 10.1021/acs.macromol.8b02701
Macromolecules 2019, 52, 2521−2530

ii. Steady Value at High W_{iR}. All blends in Figure 4a seem to reach the same steady value for all applied W_{iR}, apart from the one at the highest W_{iR} of 73. Indeed, for this particular W_{iR}, blends B1−B3 reach the same steady value, while B4 does not. This is due to the fact that as shown in Figure 8 blend B4 suffers brittle fracture at high Hencky strains, before the apparent steady state is reached. Measurements were repeated three times at this specific strain rate, and brittle fracture was observed at a similar Hencky strain for all measurements. The experimental data indicate, however, an onset of a steady state right before the fracture.

iii. Averaging of the Data at Low Strain Rates. Data measured at low strain rates (0.003 s^{-1} for all blends and 0.01 s^{-1} for blend B4) were averaged to eliminate noise. Indeed, at these low rates, the viscoelastic response of the blends was close to the sensitivity limit of the force transducer, thus leading to a significant level of noise as shown in Figure 9. As can be observed, this averaging has little effect at long times and has almost no effect on the steady value.

Measurements at very low strain rates (0.001 s^{-1}) were performed in an attempt to recreate the linear viscoelastic envelopes. However, the response from the materials turned out to be too noisy (for $\varepsilon_H > 2$), and the steady state could not be attained. It should be noted that blend B4 could not be measured at this particular rate, as the sample base viscosity was too low.

D. Modelling of the Linear Viscoelastic Data

To model the linear viscoelastic properties of the long linear chains in different oligomers/short chains matrices, we used the tube-based model (TMA) developed at UCL Louvain and followed the approach described in refs 27 and 59 in the case of binary blends with well-separated relaxation times. We summarize the main concepts here.

After the relaxation of the short chains, the long chains start to explore their dilated (fat) tube, which is only composed of long−long entanglements. These motions, which take place at the rhythm of the motion of the short chains, are well described by a constraint release Rouse process and end as soon as the long−long entanglements segments (i.e., the segments between two entanglements formed by the long chains) are relaxed. The corresponding relaxation time of these last ones is

$$\tau_{\text{long-long,ent}} = \max(\tau_{\text{obs}}, \tau_e)\left(\frac{\upsilon_1}{\upsilon_2}\right)^2 \tag{5}$$

where υ_1 and υ_2 are the weight ratio of the short chains (90 wt %) to the long chains (10 wt %), τ_e is the Rouse time of a segment between two (short or long) initial entanglements, and τ_{obs} is the average lifetime of a short long entanglement. Following ref 59, this last one can be defined as

$$\tau_{\text{obs}} = 3\frac{\tau_1}{Z_1^2} \tag{6}$$

where Z_1 and τ_1 are the initial number of entanglements and the terminal relaxation time of the short chain matrix, respectively.

The influence of the fast motion of the matrix on the contour length fluctuations of the long chains must also be taken into account. Following ref 59, when the long component is diluted in a matrix with a much lower molar mass, we consider that the fluctuations of the long components take place in a dilated (or fat) tube at the time scale of the short chains motions. Therefore, the contour length fluctuations of the molecular segments, x_{fat}, localized along the dilated tube ($x_{\text{fat}} = 0$ at the chain extremities and $x_{\text{fat}} = 1$ in the middle of the chain) are activated by the constraint release events coming from the short component, and the corresponding relaxation times are described as

$$\tau_{\text{CR-CLF}}(x_{\text{fat tube}}) = \tau_{\text{long-long,ent}}\frac{9\pi^3}{16}(\upsilon_2 Z_{\text{arm},2})^4 x_{\text{fat tube}}{}^4 \tag{7}$$

where $Z_{\text{arm},2}$ is the number of initial entanglements along half of the long chains.

In addition to CLF, the long chains can reptate. We consider that the reptation process is also taking place in a dilated tube.

On the other hand, the relaxation of the short chain matrix is described by a Rouse process (for the 8.8 matrix) or, in case that it is entangled, by considering its relaxation by contour length fluctuations, reptation, and constraint release, as is usually done.[59]

The material parameters of the models are the plateau modulus, the average molar mass between two entanglements, and the Rouse time of an entanglement segment. They have been fixed according to ref 27, i.e., equal to 230 kPa, 15 kg/mol, and 0.12 s (at a reference temperature of T_g + 31.4 °C), respectively. The relaxation times of the short matrices have been fixed to 15, 1, 0.3, and 0.014 s for the matrix in blends B1, B2, B3, and B4, respectively.

AUTHOR INFORMATION

Corresponding Author

*E-mail evelyne.vanruymbeke@uclouvain.be.

ORCID

Christian Clasen: 0000-0002-9253-9008

Evelyne van Ruymbeke: 0000-0001-7633-0194

Notes

The authors declare no competing financial interest.

ACKNOWLEDGMENTS

The authors thank Prof. Dimitris Vlassopoulos for very helpful discussions and suggestions, Dr. Meik Ranft (BASF Ludwigshafen, Germany) for the determination of molecular weight distribution of the PS820 sample, and Q. Huang for advice in sample preparation. This work was funded by DSM Materials Science Center (for T.S.), the Bijzonder Onderzoeksfonds KU Leuven (GOA 15/007) (for C.C.), and the F.N.R.S. (for E.V.R. as chercheur qualifie).

REFERENCES

(1) Hua, C. C.; Schieber, J. D. Segment connectivity, chain-length breathing, segmental stretch, and constraint release in reptation models. I. Theory and single-step strain predictions. *J. Chem. Phys.* **1998**, *109*, 10018−10027.

(2) Schieber, J. D.; Neergaard, J.; Gupta, S. A full-chain, temporary network model with sliplinks, chain-length fluctuations, chain connectivity and chain stretching. *J. Rheol.* **2003**, *47*, 213−233.

(3) Nair, D. M.; Schieber, J. D. Linear Viscoelastic Predictions of a Consistently Unconstrained Brownian Slip-Link Model. *Macromolecules* **2006**, *39* (9), 3386−3397.

(4) Khaliullin, R. N.; Schieber, J. D. Application of the slip-link model to bidisperse systems. *Macromolecules* **2010**, *43*, 6202.

(5) Masubuchi, Y.; Takimoto, J.; Koyama, K.; Ianniruberto, G.; Marrucci, G.; Greco, F. Brownian simulations of a network of reptating primitive chains. *J. Chem. Phys.* **2001**, *115* (9), 4387−4394.

DOI: 10.1021/acs.macromol.8b02701
Macromolecules 2019, 52, 2521−2530

(6) Masubuchi, Y.; Ianniruberto, G.; Greco, F.; Marrucci, G. Entanglement molecular weight and frequency response of sliplink networks. *J. Chem. Phys.* **2003**, *119* (13), 6925−6930.
(7) Masubuchi, Y.; Watanabe, H.; Ianniruberto, G.; Greco, F.; Marrucci, G. Comparison among slip-link simulations of bidisperse linear polymer melts. *Macromolecules* **2008**, *41* (21), 8275−8280.
(8) Shanbhag, S.; Larson, R. G. A slip-link model of branch-point motion in entangled polymers. *Macromolecules* **2004**, *37* (21), 8160−8166.
(9) Likhtman, A. E. Single-chain slip-link model of entangled polymers: Simultaneous description of neutron spin− echo, rheology, and diffusion. *Macromolecules* **2005**, *38* (14), 6128−6139.
(10) Andreev, M.; Khaliullin, R. N.; Steenbakkers, R. J. A.; Schieber, J. D. Approximations of the discrete slip-link model and their effect on nonlinear rheology predictions. *J. Rheol.* **2013**, *57* (2), 535−557.
(11) Shivokhin, M. E.; van Ruymbeke, E.; Bailly, C.; Kouloumasis, D.; Hadjichristidis, N.; Likhtman, A. E. Understanding Constraint Release in Star/Linear Polymer Blends. *Macromolecules* **2014**, *47* (7), 2451−2463.
(12) Doi, M.; Edwards, S. F. *The Theory of Polymer Dynamics*; Clarendon Press: Oxford, 1986.
(13) Likhtman, A. E.; McLeish, T. C. B. Quantitative theory for linear dynamics of linear entangled polymers. *Macromolecules* **2002**, *35*, 6332−6343.
(14) McLeish, T. C. B. Tube theory of entangled polymer dynamics. *Adv. Phys.* **2002**, *51*, 1379−1527.
(15) Watanabe, H. Viscoelasticity and dynamics of entangled polymers. *Prog. Polym. Sci.* **1999**, *24* (9), 1253−1403.
(16) Park, S. J.; Larson, R. G. Tube Dilation and Reptation in Binary Blends of Monodisperse Linear Polymers. *Macromolecules* **2004**, *37* (2), 597−604.
(17) van Ruymbeke, E.; Vlassopoulos, D.; Kapnistos, M.; Liu, C. Y.; Bailly, C. Proposal to Solve the Time-Stress Discrepancy of Tube Models. *Macromolecules* **2010**, *43*, 525−531.
(18) Marrucci, G. Relaxation by reptation and tube enlargement: A model for polydisperse polymers. *J. Polym. Sci., Polym. Phys. Ed.* **1985**, *23*, 159.
(19) Watanabe, H.; Ishida, S.; Matsumiya, Y.; Inoue, T. Viscoelastic and Dielectric Behavior of Entangled Blends of Linear Polyisoprenes Having Widely Separated Molecular Weights: Test of Tube Dilation Picture. *Macromolecules* **2004**, *37* (5), 1937−1951.
(20) van Ruymbeke, E.; Shchetnikava, V.; Matsumiya, Y.; Watanabe, H. Dynamic dilution effect in binary blends of linear polymers with well-separated molecular weights. *Macromolecules* **2014**, *47* (21), 7653−7665.
(21) Read, D. J.; Jagannathan, K.; Sukumaran, S. K.; Auhl, D. A full-chain constitutive model for bidisperse blends of linear polymers. *J. Rheol.* **2012**, *56* (4), 823−873.
(22) Read, D. J.; Shivokhin, M. E.; Likhtman, A. E. Contour length fluctuations and constraint release in entangled polymers: slip-spring simulations and their implications for binary blend rheology. *J. Rheol.* **2018**, *62*, 1017.
(23) van Ruymbeke, E.; Masubuchi, Y.; Watanabe, H. Effective value of the dynamic dilution exponent in bidisperse linear polymers: From 1 to 4/3. *Macromolecules* **2012**, *45* (4), 2085−2098.
(24) Ferry, J. D. *Viscoelastic Properties of Polymers*, 3rd ed.; John Wiley & Sons: New York, 1980.
(25) Yaoita, T.; Isaki, T.; Masubuchi, Y.; Watanabe, H.; Ianniruberto, G.; Marrucci, G. Primitive Chain Network Simulation of Elongational Flows of Entangled Linear Chains: Role of Finite Chain Extensibility. *Macromolecules* **2011**, *44*, 9675−9682.
(26) Huang, Q.; Hengeller, L.; Alvarez, N. J.; Hassager, O. Bridging the Gap between Polymer Melts and Solutions in Extensional Rheology. *Macromolecules* **2015**, *48*, 4158−4163.
(27) Shahid, T.; Huang, Q.; Oosterlinck, F.; Clasen, C.; van Ruymbeke, E. Dynamic dilution exponent in monodisperse entangled polymer solutions. *Soft Matter* **2017**, *13* (1), 269.
(28) Bhattacharjee, P. K.; Nguyen, D. A.; Mckinley, G. H.; Sridhar, T. Extensional stress growth and stress relaxation in entangled polymer solutions. *J. Rheol.* **2003**, *47*, 269.
(29) Bach, A.; Almdal, K.; Rasmussen, H. K.; Hassager, O. Elongational viscosity of narrow molar mass distribution polystyrene. *Macromolecules* **2003**, *36*, 5174−5179.
(30) Auhl, D.; Chambon, P.; McLeish, T. C. B.; Read, D. J. Elongational Flow of Blends of Long and Short Polymers: Effective Stretch Relaxation Time. *Phys. Rev. Lett.* **2009**, *103*, 136001.
(31) Marrucci, G.; Ianniruberto, G. Interchain pressure effect in extensional flows of entangled polymer melts. *Macromolecules* **2004**, *37*, 3934−3942.
(32) Wagner, M. H.; Rolon-Garrido, V. H. Nonlinear rheology of linear polymer melts: modeling chain stretch by interchain tube pressure and Rouse time. *Korea-Australia Rheol. J.* **2009**, *21*, 203−211.
(33) Wagner, M. H. An extended interchain tube pressure model for elongational flow of polystyrene melts and concentrated solutions. *J. Non-Newtonian Fluid Mech.* **2015**, *222*, 121−131.
(34) Wagner, M. H.; Narimissa, E.; Rolon-Garrido, V. H. From melt to solution: Scaling relations for concentrated polystyrene solutions. *J. Rheol.* **2015**, *59*, 1113−1130.
(35) Wagner, M. H. Scaling relations for elongational flow of polystyrene melts and concentrated solutions of polystyrene in oligomeric styrene. *Rheol. Acta* **2014**, *53*, 765−777.
(36) van Ruymbeke, E.; Nielsen, J.; Hassager, O. Linear and nonlinear viscoelastic properties of bidisperse linear polymers: Mixing law and tube pressure effect. *J. Rheol.* **2010**, *54*, 1155.
(37) Ianniruberto, G.; Brasiello, A.; Marrucci, G. Friction coefficient does not stay constant in nonlinear viscoelasticity. *Proc. 7th Annu. Eur. Rheol. Conf.* **2011**, *1*, 61.
(38) Ianniruberto, G.; Brasiello, A.; Marrucci, G. Simulations of Fast Shear Flows of PS Oligomers Confirm Monomeric Friction Reduction in Fast Elongational Flows of Monodisperse PS Melts As Indicated by Rheooptical Data. *Macromolecules* **2012**, *45*, 8058.
(39) Yaoita, T.; Isaki, T.; Masubuchi, Y.; Watanabe, H.; Ianniruberto, G.; Marrucci, G. Primitive chain network simulation of elongational flows of entangled linear chains: stretch/orientation-induced reduction of monomeric friction. *Macromolecules* **2012**, *45*, 2773.
(40) Huang, Q.; Alvarez, N. J.; Matsumiya, Y.; Rasmussen, H. K.; Watanabe, H.; Hassager, O. Extensional Rheology of Entangled Polystyrene Solutions Suggests Importance of Nematic Interactions. *ACS Macro Lett.* **2013**, *2*, 741−744.
(41) Deloche, B.; Samulski, E. T. Short-range nematic-like orientational order in strained elastomers: a deuterium magnetic resonance study. *Macromolecules* **1981**, *14* (3), 575−581.
(42) Thulstrup, E. W.; Michl, J. Orientation and linear dichroism of symmetrical aromatic molecules imbedded in stretched polyethylene. *J. Am. Chem. Soc.* **1982**, *104* (21), 5594−5604.
(43) Doi, M.; Watanabe, H. Effect of nematic interaction on the Rouse dynamics. *Macromolecules* **1991**, *24* (3), 740−744.
(44) Ianniruberto, G. Extensional Flows of Solutions of Entangled Polymers Confirm Reduction of Friction Coefficient. *Macromolecules* **2015**, *48*, 6306−6312.
(45) Costanzo, S.; Huang, Q.; Ianniruberto, G.; Marrucci, G.; Hassager, O.; Vlassopoulos, D. Shear and Extensional Rheology of Polystyrene Melts and Solutions with the Same Number of Entanglements. *Macromolecules* **2016**, *49*, 3925−3935.
(46) Park, G. W.; Ianniruberto, G. Flow-induced nematic interaction and friction reduction successfully describe PS melt and solution data in extension startup and relaxation. *Macromolecules* **2017**, *50*, 4787−4796.
(47) Ylitalo, C. M.; Zawada, J. A.; Fuller, G. G.; Abetz, V.; Stadler, R. Oligomers As Molecular Probes of Orientational Coupling Interactions in Polymer Melts and Networks. *Polymer* **1992**, *33*, 2949−2960.
(48) Tassin, J. F.; Baschwitz, A.; Moise, J. Y.; Monnerie, L. Relaxation of Binary Blends of Long and Short Chains - Evidence for Orientational Coupling. *Macromolecules* **1990**, *23*, 1879−1881.

DOI: 10.1021/acs.macromol.8b02701
Macromolecules 2019, 52, 2521−2530

(49) Doi, M.; Pearson, D.; Kornfield, J.; Fuller, G. Effect of nematic interaction in the orientational relaxation of polymer melts. *Macromolecules* **1989**, *22* (3), 1488−1490.
(50) McLeish, T. C. B.; Cates, M. E.; Higgins, J. S.; Olmsted, P. D.; Doi, M.; Takimoto, J.-I. Molecular modelling of entanglement. *Philos. Trans. R. Soc. London, Ser. A* **2003**, *361*, 641.
(51) Wang, Y.; Boukany, P.; Wang, S. Q.; Wang, X. Elastic breakup in uniaxial extension of entangled polymer melts. *Phys. Rev. Lett.* **2007**, *99*, 237801.
(52) Lyhne, A.; Rasmussen, H. K.; Hassager, O. Simulation of Elastic Rupture in Extension of Entangled Monodisperse Polymer Melts. *Phys. Rev. Lett.* **2009**, *102*, 138301.
(53) Wang, S. Q. *Nonlinear Polymer Rheology: Macroscopic Phenomenology and Molecular Foundation*; Wiley: Hoboken, NJ, 2017.
(54) Williams, M. L.; Landel, R. F.; Ferry, J. D. The temperature dependence of relaxation mechanisms in amorphous polymers and other glass-forming liquids. *J. Am. Chem. Soc.* **1955**, *77*, 3701.
(55) Liu, C. Y.; He, J.; Keunings, R.; Bailly, C. New linearized relation for the universal viscosity− temperature behavior of polymer melts. *Macromolecules* **2006**, *39*, 8867.
(56) Szántó, L.; Vogt, R.; Meier, J.; Auhl, D.; van Ruymbeke, E.; Friedrich, C. Entanglement relaxation time of polyethylene melts from high-frequency rheometry in the mega-hertz range. *J. Rheol.* **2017**, *61*, 1023−1033.
(57) Huang, Q.; Mednova, O.; Rasmussen, H. K.; Alvarez, N. J.; Skov, A. L.; Hassager, O. Concentrated polymer solutions are different from melts: Role of entanglement molecular weight. *Macromolecules* **2013**, *46*, 5026.
(58) Wingstrand, S. L.; Alvarez, N. J.; Huang, Q.; Hassager, O. Linear and Nonlinear Universality in the Rheology of Polymer Melts and Solutions. *Phys. Rev. Lett.* **2015**, *115*, No. 078302.
(59) Ebrahimi, T.; Taghipour, H.; Grießl, D.; Mehrkhodavandi, P.; Hatzikiriakos, S. G.; van Ruymbeke, E. Binary blends of entangled star and linear poly (hydroxybutyrate): Effect of constraint release and dynamic tube dilation. *Macromolecules* **2017**, *50* (6), 2535−2546.

DOI: 10.1021/acs.macromol.8b02701
Macromolecules 2019, 52, 2521−2530